Arabian Journal of Chemistry (2014) 7, 509–517

King Saud University

Arabian Journal of Chemistry

www.ksu.edu.sa
www.sciencedirect.com

ORIGINAL ARTICLE

Synthesis, spectroscopic, DNA cleavage and antibacterial activity of binuclear schiff base complexes

N. Mahalakshmi, R. Rajavel *

Department of Chemistry, Periyar University, Salem 636 011, Tamilnadu, India

Received 10 August 2010; accepted 25 November 2010
Available online 28 November 2010

KEYWORDS

Schiff base;
Fluorescence quenching;
CT-DNA cleavage;
Antimicrobial activity;
2-Aminobenzaldehyde;
3,3′,4,4′-tetraminobiphenyl

Abstract The binuclear Schiff base complexes are formed newly using different transition metals at their stable oxidation state as Cu(II), Ni(II), and VO(II). 3,3′,4,4′-tetraminobiphenyl and 2-aminobenzaldehyde were condensed to form a new Schiff base ligand having an two N_4 group responsible for better chelating to the metal centers. The ligand and their complexes have been established by analytical, spectral and electrochemical data. The interaction studies of the complexes with CT-DNA were carried out using cyclic voltammetry, viscosity measurements and fluorescence spectroscopy. The free ligand and their metal complexes were screened for their antimicrobial activities against the following species: *Klebsiella pneumoniae, Escherichia coli* and *Staphylococcus aureus*. A comparative study of minimum inhibitory concentration (MIC) values of the Schiff base and its complexes indicate that the metal complexes exhibit higher antibacterial activity than the free ligand.

1. Introduction

Schiff base complexes have been extensively investigated for more than a century and employed in areas that include magneto chemistry (Lu et al., 2007), non-linear optics (Di Bella and Fragala, 2002) photo physical studies (Cozzi et al., 2003) catalysis (Gianneschi et al., 2005) and materials chemistry (Morris et al., 2001). Di- and polynuclear metal complexes of transition metals (including many Schiff base complexes) have been continuing interest because of their roles as biological models, as catalysts for organic reactions, as components in the formation of new materials and/or their usefulness as structural components for the synthesis of new metallo-supramolecular structures (Yoon et al., 2004). Currently a considerable effort is being investigated in the development of new chelating ligands; particularly, the binucleating imino ligands are versatile and they exhibit very rich coordination chemistry. Such species occupy an important position in modern inorganic chemistry (Chakraborty et al., 2002; Erxleben and Hermann, 2000; Wang and Jin, 2006) and the complexing ability towards transition metals. Due to variety of applications,

* Corresponding author. Tel.: +91 9865094324; fax: +91 427 2345124.
E-mail address: drrajavel2010@rediffmail.com (R. Rajavel).
Peer review under responsibility of King Saud University.

ELSEVIER Production and hosting by Elsevier

1878-5352 © 2010 Production and hosting by Elsevier B.V. on behalf of King Saud University.
http://dx.doi.org/10.1016/j.arabjc.2010.11.010

new series of binuclear complexes of copper(II), nickel(II) and VO(II) ions with Schiff base have been synthesized. The purpose is to modify the metal ion coordination environment. This is primarily responsible for the properties exhibited by the binuclear complexes. They have attracted immense attention with the set of studies of metalloproteins (Tolman et al., 1989; Wilkins, 1992; Stassinopoules and Caradona, 1990). The major intracellular target of anticancer metallodrugs is DNA, therefore metal complexes that can bind to specific nucleobases of DNA are of interest in the development of antitumor agents. Additionally, the DNA binding efficiency can be further modified by providing multiple binding/ coordination sites in the synthesized metal complexes. It will also be useful to biologically soft metal ions and their complexes, reducing the toxic effect and enabling faster and efficient removal of the drug from the body. Binuclear copper(II) complexes show their greater cleaving efficiency or DNA interaction than mononuclear complexes. Literature search reveals that no work has been done on the condensation process of 2-aminobenzaldehyde, 3,3′,4,4′-tetraminobiphenyl. We have, therefore, undertaken the synthesis and characterization, redox, antimicrobial and DNA cleavage studies of a few bimetallic complexes formed from Cu(II), Ni(II), and VO(II) containing binuclear Schiff base derived from 2-aminobenzaldehyde and 3,3′,4,4′-tetraminobiphenyl.

2. Experimental

2.1. Materials

All the chemicals used were chemically pure and AR grade. Solvents were purified and dried according to standard procedures (Vogel, 1989). Metals were purchased from Merck. 3,3′,4,4′-tetraminobiphenyl and 2-aminobenzaldehyde were obtained from Aldrich. Synthesis: Caution! Perchlorate salts are potentially explosive and were handled only in small quantities with care.

2.2. Physical measurements

The elemental analysis were carried out with a Carlo-Erba 1106-model 240 Perkin–Elmer analyzer. The solution conductivity measurements were performed to establish the charge type of the complexes. The complexes were dissolved in CH_3CN/DMF/DMSO and molar conductivities of 10^{-3} M of their solutions at 29 °C were measured. Infrared spectra were recorded on the Perkin–Elmer FT-IR-8300 model spectrometer using KBr disc and Nujol mull techniques in the range of 4000–400 cm^{-1}. Electronic absorption spectra were recorded using Perkin–Elmer Lambda-25 in the range of 200–800 nm. EPR spectra were recorded on a Varian JEOL-JES-TE100 ESR spectrophotometer at X-band microwave frequencies for powdered samples Cyclic voltammetry studies were performed at CHI760 electrochemical analyzer, in single compartmental cells at 29 °C with H_2O/DMSO (95:5) solution using tetrabutyl ammonium perchlorate as a supporting electrolyte.

2.3. Preparation of binucleating tetradentate Schiff base ligand

The binucleating tetradentate Schiff base was prepared by condensation of tetramine with appropriate aldehydes (Scheme 1).

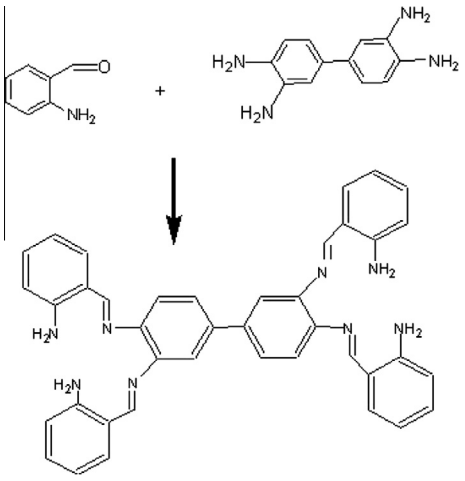

Scheme 1 Structure of binucleating tetradendate Schiff base ligand.

3,3′,4,4′-tetraminobiphenyl (0.214 g; 1 mmol) in 20 ml of methanol was stirred with 2-aminobenzaldehyde (0.42 g; 4 mmol) in

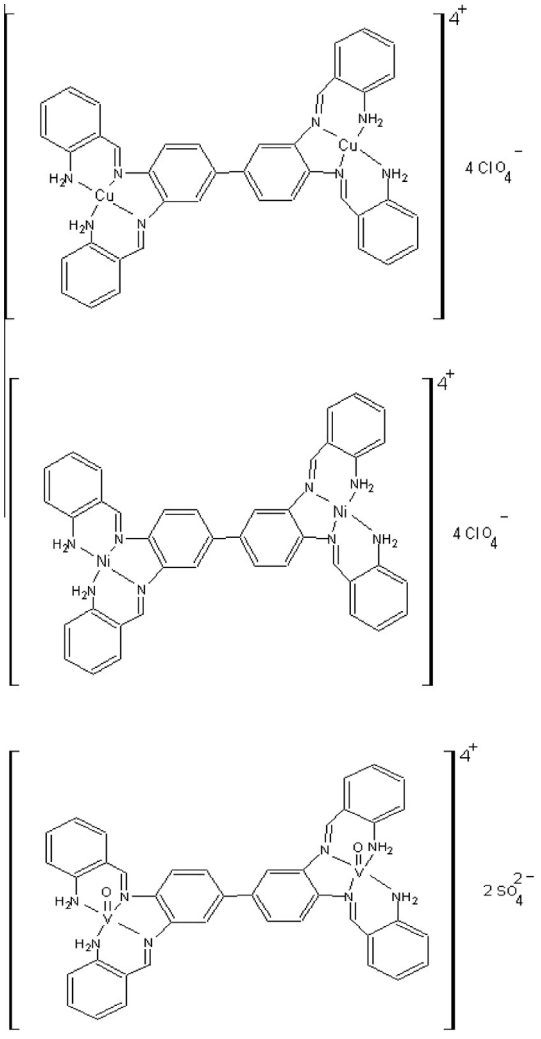

Scheme 2 Structure of binuclear Cu(II), Ni(II) and VO(II) Schiff base complexes.

Table 1 Physical characterization, analytical data of the ligand and binuclear Schiff base complexes.

Complexes	M. point	Color	Yield(%)	Found (calculated) (%)			
				M	C	N	H
($C_{40}H_{34}N_8$) (ligand)	180	Red	90	–	76.67(76.69)	17.89(17.92)	5.43(5.50)
$[Cu_2(L)]4ClO_4$	280	Brown	75	11.13(11.20)	41.74(41.79)	9.74(9.78)	2.96(2.99)
$[Ni_2(L)]4ClO_4$	235	Light green	70	10.35(10.39)	42.11(42.15)	9.82(9.85)	2.98(3.10)
$[VO_2(L)]2SO_4$	245	Dark green	65	10.70(10.73)	50.42(50.45)	11.76(11.80)	3.57(3.60)

20 ml of methanol for 2 h. The resulting red solid was separated and dried in vacuum. Yield: 80%.

2.4. Synthesis of binuclear Schiff base complexes

Metal(II) perchlorates of [Cu(II), Ni(II)] and [VO(II)] sulphate (0.2 mmol) and the potential binucleating Schiff base ligand (0.1 mmol) were dissolved in DMF (20 ml) and the mixture was heated to reflux for 4 h and the reactions were monitored by TLC. After partial evaporation of the solvent, solid (65–75%) metal(II) Schiff base complexes (Scheme 2) were separated and dried in vacuum. The analysis results are in good consistency with proposed formulas in Table 1.

2.5. Viscosity experiments

Viscosity measurements were carried out from observed flow time of CT-DNA containing solution ($t > 100$ s) corrected for the flow time of buffer alone (t_0), using Ostwald's viscometer at 29 ± 0.01 °C. Flow time was measured with a digital stopwatch. Each complex was measured three times and an average flow time was calculated. Data was presented as (η/η^0) versus binding ratio ([complex]/[DNA]) (Cohen and Eisenberg, 1969) where η is the viscosity of DNA in the presence of the complex and η^0 is the viscosity of DNA alone. Viscosity values were calculated from the equation $\eta = t - t^0$ (Eriksson et al., 1994).

2.6. Fluorescence quenching studies

Fluorescence quenching measurements were carried out using Hitachi F-2500 spectrofluorometer at 25 °C. The Tris–HCl buffer was used as blank to make preliminary adjustments. Quenching experiments were conducted by adding aliquots of $0–1.2 \times 10^{-4}$ M solutions of metal complexes to samples containing 2×10^{-5} M ethidium bromide (EB) and 0.3×10^{-4} M CT-DNA in Tris–HCl buffer. Fluorescence quenching can be described by the well-known Stern–Volmer equation is the following:

$$I_0/I = 1 + Kr\mathrm{Cu} \quad (1)$$

where I_0 and I are the emission intensity in the absence and in the presence of the complex, respectively. K is a linear Stern–Volmer quenching constant. rCu is the ratio of total concentration of the complex to that of CT-DNA.

2.7. CT-DNA cleavage study

The cleavage of CT-DNA was determined by agarose gel electrophoresis. The gel electrophoresis experiments were performed by incubation of the samples containing 40 μM CT-DNA, 40 μM metal complexes and 50 μM H_2O_2 in Tris–HCl/NaCl buffer (pH 7.2) at 30 °C for 2 h. After incubation, the samples were electrophoresed for 2 h at 50 V on 1% agarose gel using Tris–acetic acid–EDTA buffer (pH 7.2). The gel was then stained using 1 μg/cm^{-3} ethidium bromide (EB) and photographed under ultraviolet light at 360 nm. All the experiments were performed at room temperature.

2.8. Antimicrobial activity

The *in vitro* antibacterial activity of the ligand and the complexes were tested against the bacteria *Klebsiella pneumoniae, Escherichia coli* and *Staphylococcus aureus* by well diffusion method using nutrient agar as the medium. Streptomycin was used as standard for bacteria. The stock solution (10^{-2} M) was prepared by dissolving the compound in DMF and the solution was serially diluted in order to find minimum inhibitory concentration (MIC) values. In a typical procedure, a well was made on the agar medium inoculated with microorganisms in a Petri plate. The well was filled with the test solution and the plate was incubated for 24 h for bacteria at 37 °C. During the period, the test solution diffused and the growth of the inoculated microorganisms was affected. The inhibition zone was developed, at which the concentration was noted.

3. Results and discussion

The binuclear Schiff base complexes (Scheme 1) were achieved by reacting transition metals Cu(II), Ni(II) and VO(II) with binucleating tetradendate Schiff base ligand. The Schiff base ligand has been synthesized from 2-aminobenzaldehyde and 3,3′,4,4′-tetraminobiphenyl (Scheme 1) ($C_{40}H_{34}N_8$), in 2:1 mole ratio. The analysis of the complexes were consistent with the stoichiometry proposed and are summarized in Table 1. The data in consistent with the earlier reports support the proposed formulation of the binuclear complexes (Scheme 2). The higher conductance values Table 2 of chelates support the electrolytic (1:2) nature of metal complexes. The new binuclear complexes

Table 2 Molar conductance data of the binuclear Schiff base complexes.

Complexes	Solvent	Molar conductance Λ_m (ohm^{-1} cm^2 mol^{-1})	Types of electrolyte
$[Cu_2(L)]4ClO_4$	MeCN	280	1:2
	DMF	240	1:2
$[Ni_2(L)]4ClO_4$	MeCN	120	1:2
	DMSO	125	1:2
$[VO_2(L)]2SO_4$	MeCN	164	1:2
	DMSO	142	1:2

are stable, hygroscopic with higher melting points, insoluble in water, soluble in acetonitrile, chloroform, DMF and DMSO producing intense color in their solutions.

3.1. IR spectra

Vibrational spectra provide valuable information regarding the nature of functional group attached to the metal ion in the complexes. The IR spectra of the Schiff base ligand data showed in Table 3, a broad band in the region 3480–3466 cm^{-1} indicating the presence of NH_2 group. On complexation this band is shifted to lower frequency in the range (3430–3452 cm^{-1}) shows the involvement of primary amine nitrogen in coordination to metal ion for all the Schiff base complexes (Ray et al., 2009). The azomethine nitrogen υC=N stretching frequency of the free ligand appears 1602 cm^{-1}, which is shifted to lower frequencies in the spectra of all the complexes (1584–1590 cm^{-1}). These bands are shifted to lower wave numbers indicating the involvement of azomethine nitrogen in coordination to the metal ion (Abdel-Latif et al., 2007). Accordingly, the ligand acts as a tetradendate chelating agent, bonded to the metal ion via two primary amine and two azomethine nitrogen atoms of the Schiff base (Scheme 2). Assignment of the proposed coordination sites is further supported by the appearance of medium bands at 450–480 cm^{-1} which could be attributed to υM–N, respectively (Thomas et al., 1995; Nakamoto, 1997). In addition, the vanadyl complexes show a band at 980 cm^{-1} attributed to V=O stretching frequency (Xiu et al., 1996). A further examination of Infrared spectra of the complexes shows the presence of a band in the 1070–1110 cm^{-1} region. The strong band is ascribable to ClO_4^- and SO_4^{2-} ions (Nakamoto, 1978).

3.2. Electronic spectra

The UV–Visible spectrum of the Schiff base ligand and its complexes were recorded in DMF solution in the range of 200–800 nm regions and the data are presented in Table 4. The absorption spectrum of free ligand consists of an intense band centered at 330 nm attributed to n–π^* transitions of the azomethine group. Another intense band in higher energy region of the spectra of the free ligand was related to $\pi \rightarrow \pi^*$ transitions of benzene rings. These transitions are also found in the spectra of the complexes, but they shifted towards lower frequencies, confirming the coordination of the ligand to the metal ions. Further, the d–d transition showed a strong band at 540 nm for Cu(II) complex Fig. 1. This is due to $^2B_1g \rightarrow {}^2A_1g$ transition. The spectra of Ni(II) complex in the visible region at about 510 and 488 nm is assigned to, $^1A_1g \rightarrow {}^1A_2g$, $^1A_1g \rightarrow {}^1B_1g$, transitions, suggesting an approximate square planar geometry of the ligand around the metal ions (Feigl, 1949). The intense charge transfer band at 500 and 530 nm in VO(II) complex assigned to $^2B_2 \rightarrow {}^2A_1$, $^2B_2 \rightarrow {}^2E$ transitions. This is due to electron delocalization over whole molecule on complexation. Based on these data, a square planar geometry has been assigned to the complexes except VO(II) complex which has square pyramidal geometry. These values are comparable with other reported complexes (Warad et al., 2000).

Table 3 Infrared spectral data for the ligand and binuclear Schiff base complexes.

Complexes	NH_2 (cm^{-1})	–C=N (cm^{-1})	V=O (cm^{-1})	M–N (cm^{-1})	ClO_4^-/SO_4^{2-} (cm^{-1})
($C_{40}H_{34}N_8$) (ligand)	3480	1602	–	–	–
$[Cu_2(L)]4ClO_4$	3430	1587	–	460	1090
$[Ni_2(L)]4ClO_4$	3390	1590	–	470	1110
$[VO_2(L)]2SO_4$	3362	1585	980	450	1070

Table 4 Absorption spectral data of the ligand and binuclear Schiff base complexes.

Complexes	Absorption (λ_{max} and nm)		
	d–d	$\pi \rightarrow \pi^*$ benzene/imino	$n \rightarrow \pi^*$ azomethine
($C_{40}H_{34}N_8$) ligand	–	283,250	330
$[Cu_2(L)]4ClO_4$	540	278,249	320
$[Ni_2(L)]4ClO_4$	488 510	270,242	324
$[VO_2(L)]2SO_4$	500 530	270,242	324

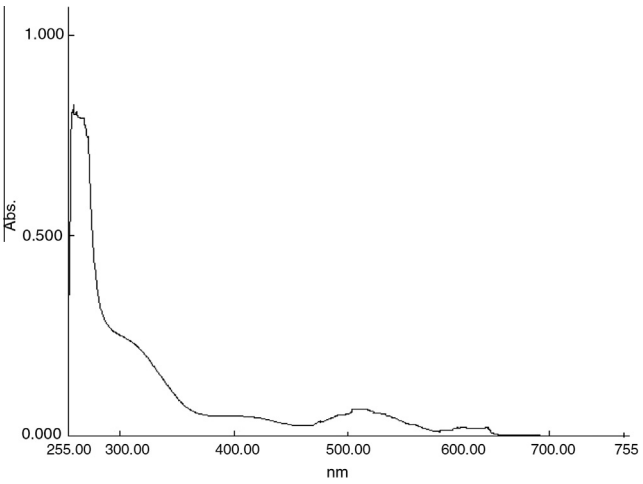

Figure 1 Absorption spectra of the binuclear Cu(II) Schiff base complex $[Cu_2(L)]ClO_4$.

3.3. ESR spectrum

The ESR spectra of metal complexes provide information about hyperfine and superhyperfine structures, which are of importance in studying the metal ion environment in the complex, i.e., the geometry, nature of ligating sites of Schiff base and metal, and the degree of covalency of metal–ligand bonds. The ESR spectra of the complexes exhibit a set of four well-resolved signals at low field and one or two signals at high field, corresponding to $g_{||}$ and $g_{\perp}$, respectively. The $g_{||}$ and $g_{\perp}$ values were computed from the spectrum using tetracyanoethylene (TCNE) free radical as the 'g' marker (2.0027). The spectrum of $[Cu_2(L)]4ClO_4^-$ is given in Fig. 2 exhibits a broad $g_{\perp}$ component, with splitting of $g_{||}$ component, reflecting the coupling with the Cu(II) nucleus ($I = 3/2$), the $g_{||}$ value at 2.10 and $g_{\perp}$ at 2.02 (Kivelson and Nieman, 1961) have reported that $g_{||}$ is less than 2.3 for covalent character and greater than 2.3 for ionic character of the metal ligand bond in the complexes. As

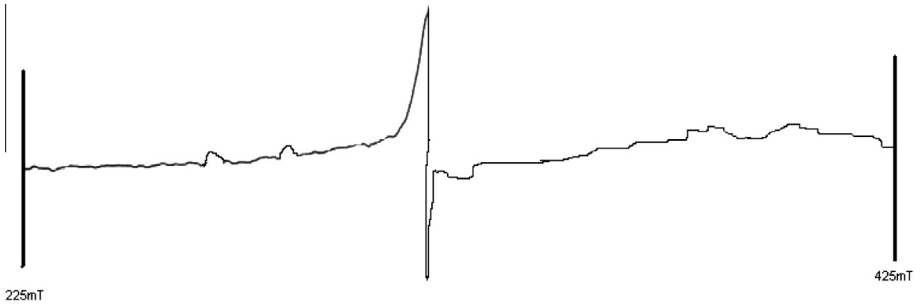

Figure 2 X-band ESR spectra of binuclear Cu(II) Schiff base complex $[Cu_2(L)]ClO_4$ at room temperature.

seen in Table 5, the $g_{||}$ value for $[Cu_2(L)]4ClO_4^-$ is less than 2.3, suggesting significant covalent character in the metal ligand bonding. The presence of $g_{||} > g_{\perp}$ is evidence for square planar geometry around copper(II) atom (Sakata et al., 1997). The axial symmetry parameter (G) value of Cu(II) complex (<4) shows that the exchange interaction is negligible. The EPR spectra of the present binuclear Cu(II) Schiff base complex is similar in nature to those of the mononuclear complex. This indicates that the two paramagnetic centers are equivalent and there is no super exchange interaction between the two metal centers. However, the Cu(II) complex is dimer with the unpaired electron lies in the $d_{x^2y^2}$ orbital. The pairing of electrons is prevented by the distance between two Cu(II) atoms provided by the bridging bis-tetradentate Schiff base ligand. From the order $g_{||} > g_{\perp} > 2.0023$, it is clear that the ground state of Cu(II) is predominantly $d_{x^2-y^2}$. The observed values of Vanadyl complex $g_{||} = 2.03 > g_{\perp} = 1.98$ indicates that the unpaired electron is present in the d_{xy} orbital with square pyramidal geometry around the VO(II) chelates (Leelavathy et al., 2009).

3.4. Cyclic voltammetry studies

The electrochemical techniques are the most effective and versatile methods available for the mechanistic study of redox systems. Cyclic voltammetry (CV) has been employed to study the interaction of the complex with CT-DNA, with a view to further explore the DNA binding modes assessed from the absorption, emission and viscometric studies. The cyclic voltammogram of complex **1** in the absence of CT-DNA is shown in Fig. 3(a) reveals non-Nernstain but fairly reversible/quasi-reversible one electron redox process involving Cu(II)/Cu(I) couple. The cyclic voltammograms of the complexes were obtained in H_2O/DMSO (95:5) solution, at scan rate 0.2 Vs^{-1} over a potential range from +1.2 to −2.0 V. In the absence of CT-DNA, complex **1** and other complexes data are listed in Table 6. The anodic peak potential (*Epa*) of complex **1** appeared at –0.432 V and the cathodic (*Epc*) at –1.292 V. The cyclic voltammograms of complex **1** reveals a one electron quasirreversible wave attributed to the redox couple Cu(II)/Cu(I), $\Delta Ep = +0.860$ V which is larger than the Nernstian value observed for the one electron transfer couple. On addition of CT-DNA, the complex **1** Fig. 3(b) shows a shift in *Epc* = (−1.213 V), *Epa* = (−0.512 V) and ΔEp = (+0.701 V) values indicating strong binding of binuclear complex with CT-DNA. The decrease in ratio of anodic to cathodic peak currents signify that adsorption of Cu(I) is enhanced in the presence of CT-DNA (Yang et al., 2004). Further, the shift in E^0 value and increase in peak height potentials suggest that both Cu(II) and Cu(I) form of complex **1** bind to CT-DNA (Mahadevan and Palaniandavar, 1998). The ratio of equilibrium constants K_+/K_{2+} for the binding of Cu(II) and Cu(I)

Table 5 ESR spectral data of the binuclear Schiff base complexes.

Complexes	$g_{\|\|}$	$g_{\perp}$	g_{iso}	G
$[Cu_2(L)]4ClO_4$	2.10	2.04	2.12	2.59
$[VO_2(L)]2SO_4$	2.03	1.98	2.04	−0.81

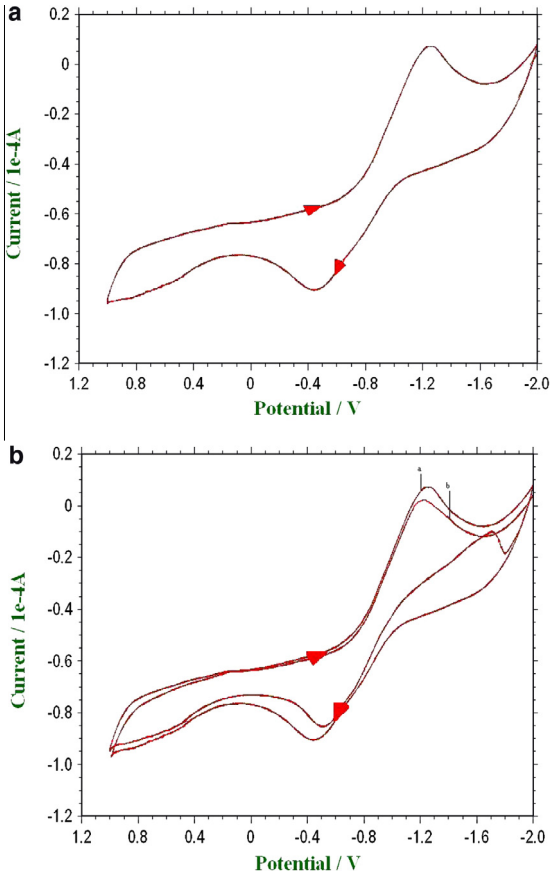

Figure 3 Cyclic voltammogram (scan rate 0.2 V s^{-1}, DMSO, 25 °C, pH 7.5) of **3.** (a) Complex **1** alone **3.** (b) Complex **1** in presence of CT-DNA [Complex **1**] 1×10^{-3} M, [DNA] 6×10^{-3} M.

Table 6 Cyclic voltammetric data of the binuclear Schiff base complexes in DMSO solution.

Complexes	Couple	*Epc* (V)	*Epa* (V)	Δ*Ep* (mv)
$[Cu_2(L)]4ClO_4$	Cu(II)/Cu(I)	−1.292	−0.432	0.860
$[Ni_2(L)]4ClO_4$	Ni(II)/Ni(I)	1.50	1.79	0.29
$[VO_2(L)]2SO_4$	VO(IV)/VO(III)	0.51	0.65	0.14
	VO(IV)/VO(V)	−1.51	−0.61	0.90

forms of complex **1** to CT-DNA have also been calculated using the following equation (Scheme 3):

$$E_b^0 - E_f^0 = 0.059\log(K_+/K_{2+}) \quad (2)$$

where E_b^0 and E_f^0 are the formal potentials of Cu(II)/Cu(I) couple in the free and bound species, respectively. The ratio of binding constant is equal to 1, K_+/K_{2+} suggesting that both Cu(II) and Cu(I) forms interact with CT-DNA to the same extent (Lu et al 2002).

3.5. Viscometry studies

To obtain further support for binding modes of the complexes with DNA, viscosity measurements were carried out as hydrodynamic measurements sensitive to length changes are regarded as the most critical tests of a binding model in solution in the crystallographic structural data (Satyanarayana et al., 1993). For DNA binding of a complex, a partial or a non-classical mode of binding could bend or kink the DNA helix, reduce its effective length and concomitantly its viscosity (Vaidyanathan and Nair, 2005). The effect of complex **1** on the viscosity of CT-DNA is shown in Fig. 4. The relative specific viscosity decreases steadily, which implies complexes bind to CT-DNA (Liu et al., 2002).

The changes in specific relative viscosity of DNA on addition of increasing concentrations of complex **1** are shown in Fig. 4. The decrease in relative viscosity of DNA observed for complex **1** suggests covalent binding of complex **1** with CT-DNA, which produced bends or kinks in the DNA and thus reduced its effective length and concomitantly its viscosity. These results are consistent observed hyperchromic effect of complex **1** bound to CT-DNA covalently.

3.6. Fluorescence spectroscopic studies

To exclude the possibility of intercalative binding mode an ethidium bromide (EB) assay was carried out. Ethidium bromide is a conjugate planar intercalating molecule emitting intense fluorescence when bound to DNA (Li et al., 2005). Decrease in emission intensity results when a second DNA

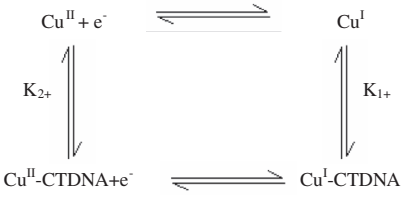

Scheme 3

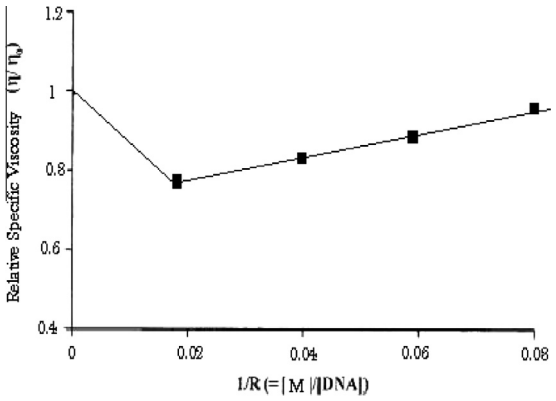

Figure 4 Effects of increasing amount of complex **1** (•) on the relative viscosity of CT-DNA at 29 ± 0.01 °C, [DNA] = 4×10^{-4} M, pH 7.2.

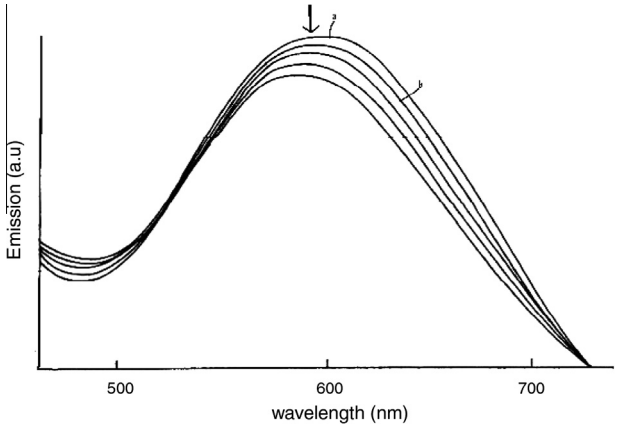

Figure 5 (a) Emission spectra of EB bound to DNA in the presence of complex **1** in Tris–HCl buffer [EB] = 2×10^{-5} M, [DNA] = 0.3×10^{-4} M, [complex] = $0–1.2 \times 10^{-4}$ M, λ_{ex} = 510 nm, λ_{em} = 600 nm. (b) The arrow indicates decreasing absorbance with increasing Cu(II) complex (Fig. 6) concentrations.

binding molecule either replaces EB or accepts the excited state electron from EB (Selvakumar et al., 2006). Complex **1** does not display luminescence either alone or in tris buffer. The addition of complex **1** to EB-DNA system resulted in the reduction of emission intensity (Fig. 5). As complex **1** bind to DNA primarily via surface binding, they cannot displace the strongly DNA bound EB. So the observed quenching occurs through the photoelectron transfer mechanism (Selvi et al., 2005). The smaller quenching extent is observed as the reduction of DNA-bound complex **1** ($E_{1/2}$ = −0.862 V), indicates low binding affinity and slight decrease in emission intensity is observed for the complex **1** with CT-DNA.

The relative fluorescence intensity, plotted as a function of CT-DNA concentration (in terms of [*M*]/[DNA]) (Fig. 6) is in good agreement with the linear Stern–Volmer Eq. (1), which also proves that the complex binds to DNA. The value of the fluorescence quenching constant *Ksv* obtained from the slope I_0/I vs r (= [complex]/[DNA]) for complex **1** is found to be 0.14.

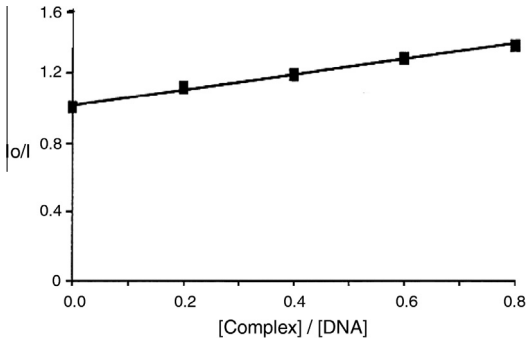

Figure 6 Fluorescence quenching curve of DNA bound EB by complex **1** (•). [EB] = 2×10^{-5} M, [DNA] = 0.3×10^{-4} M, [complex] = $0.2-1.2\times10^{-4}$ M, λ_{ex} = 510 nm, λ_{em} = 600 nm.

3.7. DNA cleavage studies

The DNA cleavage ability of the complexes is monitored by gel electrophoresis. All the metal complexes are able to convert super coiled DNA into open circular DNA. The DNA cleavage activities of the complexes are obviously concentration-dependent. With the increase of complex concentration, the super coiled DNA decreases and open circular DNA gradually increases. The results of DNA cleavage are given in Fig. 7. The general oxidative mechanisms proposed on account of DNA cleavage by hydroxyl radicals via abstraction of a hydrogen atom from sugar units predicts the release of specific residues arising from transformed sugars, depending on the position from which the hydrogen atom is removed (Prativel et al., 1991). The DNA cleavers involve oxidative destruction of the DNA deoxyribose backbone by hydrogen abstraction (Chittari et al., 1998) or alkylation's of DNA bases and, in few cases, metal activated hydrolytic cleavage of the phosphodiester linkages of DNA (Hashimoto and Nakamura, 1996) that the cleavage is inhibited by free radical scavengers, implying that hydroxyl radical or peroxy derivatives mediate the cleavage reaction. The reaction is modulated by a metallo complex bound hydroxyl radical or a peroxo species generated from the co-reactant H_2O_2. This results in oxidative attack on the deoxyribose moiety at C-1 hydrogen, leading to a series of elimination reactions that ruptures the phosphodiester backbone.

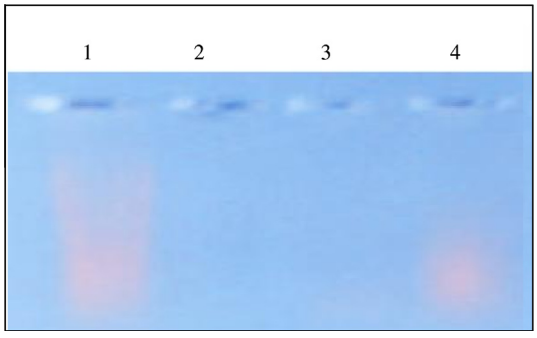

Figure 7 Changes in the agarose gel electrophoretic pattern of calf-thymus DNA induced by H_2O_2 and metal(II) complexes, Lane 1, DNA alone; Lane 2, DNA + Cu(II) complex + H_2O_2; Lane 3, Ni(II) complex + H_2O_2; Lane 4, DNA + VO(IV) complex + H_2O_2.

The greater cleavage efficiency of complexes compared to that of the control experiments is due to their efficient DNA-binding ability. Control experiments using DNA alone do not show any significant cleavage of CT-DNA even after a longer exposure time. This result revealed that the damage of DNA in Cu(II), Ni(II) and VO(II) complexes could be attributed to the cleavage of DNA. The Cu(II), Ni(II) complexes have more activity than VO(II) complex with CT-DNA. The results indicate the important role of metal complexes in this CT-DNA cleavage reaction is shown in Fig. 7. The oxidative DNA cleavage by singlet oxygen is likely to proceed via oxidation of guanine nucleobase (Erkkila et al., 1999; Croke et al., 1993).

3.8. Antimicrobial activity

Mainly the aim of production and synthesis of antimicrobial compound is to inhibit the causal microbe without any side effects on the patients. In addition, it is worthy to stress here on the basic idea of applying any chemotherapeutic agent which depends essentially on the specific control of only one biological function and not multiple ones. Cu(II),Ni(II) and VO(II) complexes show a remarkable biological activity against different types of Gram-positive (G+) and Gram-negative (G−) bacteria. These complexes are inhibiting Gram-positive and Gram-negative bacterial strains. The importance of this unique property of the investigated Schiff base complexes lies in the fact that, it can be applied safely in the treatment of infections and some common diseases e.g. septicaemia, gastroenteritis, urinary tract infections and hospital acquired infections. The ligand and their complexes have been tested for in vitro growth inhibitory activity against gram-positive microbe *S. aureus* and Gram-negative microbe's *K. pneumonia, E. coli* by using well-diffusion method. As the test solution concentration increases, the biological activity also increases. The minimum inhibitory concentration (MIC) values of the investigated compounds are summarized in Table 7. From the table, the observed MIC values indicate that the complexes have higher antimicrobial

Table 7 Antibacterial activity of the ligand and binuclear Schiff base complexes.

Complexes	*Klebsiella pneumoniae* (mm)				*Escherichia coli* (mm)				*Staphylococcus aureus* (mm)			
	25µl	50µl	75µl	100µl	25µl	50µl	75µl	100µl	25µl	50µl	75µl	100µl
$(C_{40}H_{34}N_8)$	10	11	12	14	10	12	13	15	11	13	14	16
$[Cu_2(L)]4ClO_4$	11	12	15	17	11	13	15	16	12	14	15	16
$[Ni_2(L)]4ClO_4$	11	16	17	18	11	13	16	18	12	14	17	19
$[VO_2(L)]2SO_4$	12	14	16	18	14	16	17	18	12	14	17	19

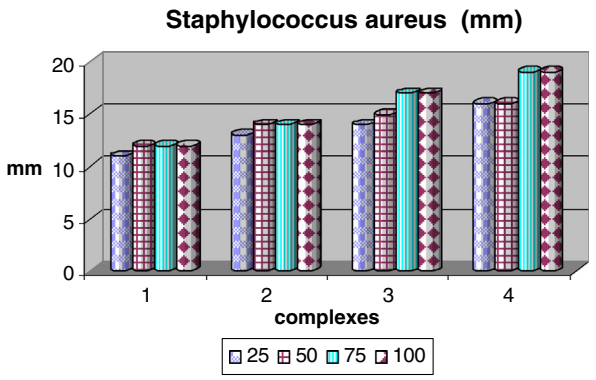

Figure 8a Difference between the antimicrobial activity of binuclear ligand and metal complexes (1)ligand($C_{40}H_{34}N_8$), (2) $[Cu_2(L)]4ClO_4$, (3) $[Ni_2(L)]4ClO_4$, (4) $[VO_2(L)]2SO_4$ [*X* axis – zone of inhibition (mm)].

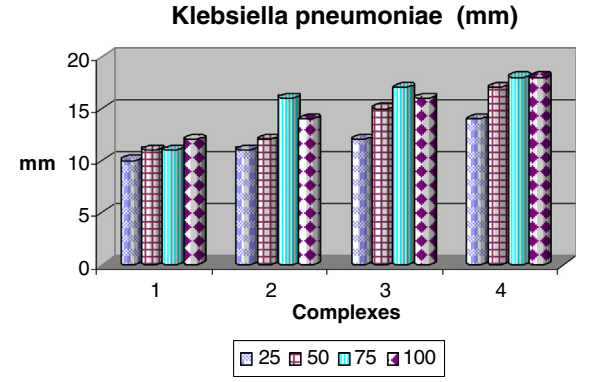

Figure 8b Difference between the antimicrobial activity of binuclear ligand and metal complexes (1) ligand ($C_{40}H_{34}N_8$), (2) $[Cu_2(L)]4ClO_4$, (3) $[Ni_2(L)]4ClO_4$, (4) $[VO_2(L)]2SO_4$. [*X* axis – zone of inhibition (mm)].

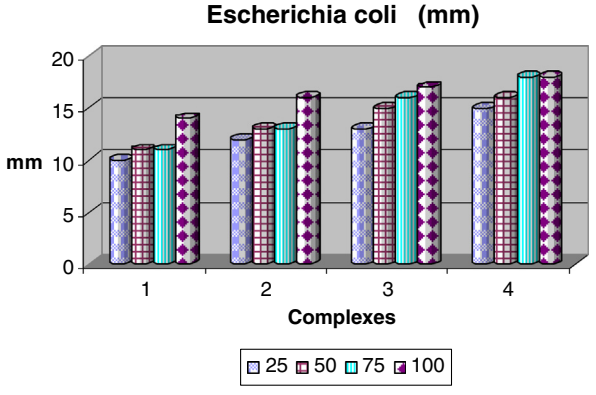

Figure 8c Difference between the antimicrobial activity of binuclear ligand and metal complexes (1) ligand ($C_{40}H_{34}N_8$), (2) $[Cu_2(L)]4ClO_4$, (3) $[Ni_2(L)]4ClO_4$, (4) $[VO_2$ (L)$]2SO_4$. [*X* axis – zone of inhibition (mm)].

activity. The metal complexes Cu(II), Ni(II) and VO(II) have higher antimicrobial activity than the ligand are shown in Fig. 8a–c. These complexes also disturb the respiration process of the cell and thus block the synthesis of proteins, which restricts further growth of the organisms. The increase in antimicrobial activity is due to the faster diffusion of metal complexes as a whole. Such increased activity of metal complexes can be explained by the chelation theory (Raman, 2005). Chelation reduces the polarity of metal atom mainly because of partial sharing of its positive charge with the donor groups and possible pi electron delocalization within the whole chelate ring. Also chelation increases the lipophilic nature of the central metal atom which subsequently favors it permeation through the lipid layer of the cell membrane.

4. Conclusions

In this work new Schiff base and their binuclear metal complexes were designed and synthesized. The spectroscopic and analytical data of binuclear complexes resulting from the reaction between 2-aminobenzaldehyde, 3,3′,4,4′-tetraminobiphenyl and Cu(II), Ni(II) and VO(II) (perchlorates, sulphate) form complexes of composition $[(M_2L)X](X = ClO_4^-$ and $SO_4^{2-})$ where *L* is the binucleating tetradendate Schiff base ligand. The IR, UV and EPR spectral results revealed that the metal complexes Cu(II), Ni(II) and VO(II) have square planar geometries and square pyramidal geometry. The interaction of these complexes with CT-DNA was investigated by gel electrophoresis. All the transition metal complexes have higher activity than the control CT-DNA. The Cu(II), Ni(II) complexes have more activity than VO(II) complex and the control CT-DNA. The metal complexes have higher antimicrobial activity than the free ligand by the chelation theory.

References

Abdel-Latif, S.A., Hassib, H.B., Issa, Y.M., 2007. Spectrochim. Acta A 67, 950–957.
Chakraborty, S., Laye, R.H., Paul, R.L., Gonnade, R., Puranik, V.G., Ward, M.D., Lahiri, G.K., 2002. J. Chem. Soc., Dalton Trans., 1172–1179.
Chittari, P., Jadhav, V.R., Ganesh, K.N., Rajappa, S.J., 1998. J. Chem. Soc. Perkin Trans. 1, 1319–1324.
Cohen, G., Eisenberg, H., 1969. Biopolymers 8, 45–55.
Cozzi, P.G., Dolci, L.S., Garelli, A., Montalti, M., Prodi, L., Zaccheroni, N., 2003. New J. Chem. 27, 692–697.
Croke, D.T., Perrouault, L., Sari, M.A., et al., 1993. J. Photochem. Photobiol. B 18, 41–50.
Di Bella, S., Fragala, I., 2002. New J. Chem. 26, 285–290.
Eriksson, M., Leijon, M., Hiort, C., Norden, B., Graslund, A., 1994. Biochemistry 33, 5031–5040.
Erkkila, K.E., Odom, D.T., Barton, J.K., 1999. Chem. Rev. 99, 2777–2796.
Erxleben, A., Hermann, J., 2000. J. Chem. Soc., Dalton Trans., 569–575.
Feigl, F., 1949. Chemistry of Specific Selective and Sensitive Reactions. Academic Press.
Gianneschi, N.C., Nguyen, S.T., Mirkin, C.A., 2005. J. Am. Chem. Soc. 127, 1644–1645.
Hashimoto, S., Nakamura, Y., 1996. J. Chem. Soc, Perkin Trans. 1, 2623–2628.
Kivelson, D., Nieman, R., 1961. J. Chem. Phys. 35, 149–155.
Leelavathy, L., Anbu, S., Kandaswamy, M., Karthikeyan, N., Mohan, N., 2009. Polyhedron 28, 903–910.
Li, H., Le, X.Y., Pang, D.W., Deng, H., Xu, Z.H., Lin, Z.H., 2005. J. Inorg. Biochem. 99, 2240–2247.

Liu, J., Lu, T.B., Li, H., Zhang, Q., Ji, L.N., Zhang, T.X., Qu, L.H., Zhou, H., 2002. Transition Met. Chem. 27, 686–690.
Lu, X., Zhu, K., Zhang, M., Liu, H., Kang, J., 2002. J. Biochem. Biophys. Methods 52, 189–200.
Lu, J.W., Huang, Y.H., Lo, S.I., Wei, H.H., 2007. Inorg. Chem. Commun. 10, 1210–1213.
Mahadevan, S., Palaniandavar, M., 1998. Inorg. Chem. 37, 693–700.
Morris, G.A., Zhou, H., Stern, C.L., Nguyen, S.T., 2001. Inorg. Chem. 40, 3222–3227.
Nakamoto, K., 1978. Infrared and Raman Spectra of Inorganic and Coordination Compounds, third ed. John Wiley.
Nakamoto, K., 1997. Inorganic and Raman Spectra of Inorganic and Coordination Compounds, 3rd ed. John Wiley, New York.
Prativel, G., Pitie, M., Bernadou, J., Meunier, B., 1991. Angew. Chem., Int. Ed. Engl. 30, 702–704.
Raman, N., 2005. Res. J. Chem. Environ. 9, 79–80.
Ray, Laurie, Georgina Rosair, M., kadam, Ramakant, Mitra, Samiran, 2009. Polyhedron 28, 796–806.
Sakata, K., Hashimoto, M., Kashiwamura, T., Tsuge, A., 1997. Synth. React. Inorg. Met. Org. Chem. 27, 797–809.
Satyanarayana, S., Dabrowiak, J.C., Chaires, J.B., 1993. Biochemistry 32, 2573–2584.
Selvakumar, B., Rajendiran, V., Maheswari, P.V., Evans, H.S., Palanaindavar, M., 2006. J. Inorg. Biochem. 100, 316–330.
Selvi, P.T., Evans, H.S., Palanaindavar, M., 2005. J. Inorg. Biochem. 99, 2110–2118.
Stassinopoules, A., Caradona, J., 1990. J. Am. Chem. Soc. 112, 7071–7079.
Thomas, M., Nair, M.K.M., Radhakrishnan, R.K., 1995. Synth. React. Inorg. Met.-Org. 25, 471–479.
Tolman, W.B., Bino, A., Lippard, S.J., 1989. J. Am. Chem. Soc. 111, 8522–8523.
Vaidyanathan, V.G., Nair, B.U., 2005. Dalton Trans. 17, 2842–2848.
Vogel, A.I., 1989, fifth ed.. In: Text Book of Practical Organic Chemistry, vol. 43 Longman, London.
Wang, W.H., Jin, G.X., 2006. Inorg. Chem. Commun. 9, 548–550.
Warad, D.U., Satish, C.D., Kulkarini, V.H., Bajgur, C.S., 2000. Ind. J. Chem. 39A, 415–420.
Wilkins, R.G., 1992. Chem. Soc. Rev., 171–178.
Xiu, R.B., Mintz, F.L., You, X.Z., Wang, R.X., Yue, Q., Meng, Q.J., Lu, Y.J., Derveer, D.V., 1996. Polyhedron 15, 4585–4591.
Yang, Z.S., Wang, Y.L., Zhao, G.C., 2004. Anal. Sci. 20, 1127–1130.
Yoon, I., Narita, M., Shimizu, T., Asakawa, M., 2004. J. Am. Chem. Soc. 126, 16740–16741.